

See discussions, stats, and author profiles for this publication at: <https://www.researchgate.net/publication/252845389>

A variant of the Titius–Bode Law

Article in *Revista mexicana de astronomía y astrofísica* · April 2011

CITATIONS

2

READS

222

2 authors, including:



[Daniel Flores](#)

Universidad Nacional Autónoma de México

19 PUBLICATIONS 24 CITATIONS

[SEE PROFILE](#)

Some of the authors of this publication are also working on these related projects:



Diseño de Metodologías y Técnicas de Registro, de Diagnóstico de Conservación y de Estrategias de Preservación y Protección del Patrimonio Rupestre de México [View project](#)

A VARIANT OF THE TITIUS-BODE LAW

J. Daniel Flores-Gutiérrez¹ and Carlos García-Guerra²

Received 2010 June 28; accepted 2011 February 15

RESUMEN

En el estudio de la distribución geométrica de los planetas invariablemente se menciona la ley de Titius Bode como un intento de clasificar *grosso modo* sus distancias heliocéntricas mediante una sucesión de números enteros. Con el descubrimiento de un gran número de objetos planetarios ahora se sustenta, en cierta medida, el principio básico de dicha ley al través de la determinación de más elementos orbitales. Abordamos brevemente una clasificación de los parámetros orbitales utilizando la constante de proporcionalidad de Kepler y discutimos el problema de la aplicación de la ley TB a sistemas extrasolares. También analizamos las funciones propuestas por diversos autores las cuales reproducen las distancias heliocéntricas de los planetas, y efectuamos una comparación con la variante a la ley Titius Bode que proponemos aquí.

ABSTRACT

The study of the geometric distribution of the planets invariably mentions the Titius Bode law as an attempt to classify their heliocentric distances through a succession of integer numbers. With the discovery of more planetary objects better support is given to the basic principle of the law through their orbital parameters. We briefly refer to a classification of orbital parameters using Kepler's proportionality parameter and discuss the problem of applying the TB Law to extrasolar systems. We also review work by various authors who have proposed functions which reproduce with some degree of certainty the planetary heliocentric distances, and we compare them to our variant of the Titius-Bode Law.

Key Words: planets and satellites: formation — planets and satellites: general — solar system: general

1. INTRODUCTION

In the late eighteenth century Johann Daniel Titius proposed a numerical sequence with which he tried to reproduce the heliocentric distances of the planets, and which was included in the compendium *Contemplation of the Nature* written by Charles Bonnet in 1764. In 1772 the famous German astronomer Johann Bode included Titius' ideas (*Latin conversion of Tietz*) in his texts on astronomy. According to Titius' scheme, the mathematical formulation is written in terms of the parameter N given by the integers 0, 3, 6, 12, 24, 48, 96 and 192 according to the order of the planets Mercury, Venus, Earth, Mars, Jupiter, Saturn and Uranus.

In terms of powers of two (2^n), the orbital parameters are determined by the equation $R_n = 4 + 3 \cdot 2^n$ where $N = -\infty, 0, 1, 2, 3, \dots$, also in the order of the planets (Nieto 1970) or as proposed most recently $R_n = 0.4 + 0.3 \cdot 2^{n-2}$ with $n = 1, 2, 3, \dots$ (Holton & Brush 2001). An interesting historical analysis of the progression was presented by Jaki (1972). Many discussions have arisen around the Titius-Bode model like those of Ovenden (1972, 1975) who analyzed the evolution of the circular and elliptical orbits and found that a Titius-Bode planetary distribution is a distribution of least interaction action between the planets, as well as how they evolve numerically into a resonant system from arbitrary initial conditions of position and velocity. Nieto (1970, 1975) made a detailed study of the Titius-Bode Law, and Horedt, Pop, & Ruck (1977) described a numerical application of the generalized Titius law for more than nine

¹Instituto de Astronomía, Universidad Nacional Autónoma de México, México.

²Facultad de Arquitectura, Universidad Nacional Autónoma de México, México.

TABLE 1

EMPIRICAL SERIES REPRODUCING THE HELIOCENTRIC DISTANCES OF THE PLANETS

MODIFIED TITIUS BODE LAW										
This Paper		This paper			a AU	T Year	a_p AU	T_p Year	Δa_n %	ΔT_n %
Body	TB N	TBmod X	X'	N'						
Mercury	0	0	0	0	0.4	0.253	0.387	0.251	3.4	0.8
Venus	3	0	3	3	0.7	0.586	0.723	0.615	-3.2	-4.8
Earth	6	3	3	6	1.0	1.000	1.000	1.000	0.0	0.0
Mars	12	6	6	12	1.6	2.024	1.523	1.881	5.0	7.6
Ceres	24	12	12	24	2.8	4.685	2.765	4.600	1.2	1.9
Jupiter	48	24	24	48	5.2	11.858	5.202	11.862	-0.1	-0.0
Saturn	96	48	48	96	10.0	31.623	9.510	29.458	5.2	7.3
Uranus	192	96	96	192	19.6	86.773	19.25	84.013	1.8	3.3
Neptune		192	96	288	29.2	157.788	30.19	164.749	-3.3	-4.2
Pluto		288	96	384	38.8	241.684	39.50	247.492	-1.8	-2.3

TB is the original succession N defining the Titius-Bode law. TBmod is the modified TB law by means of the empirical succession X and X' and $N' = X + X'$. In Columns a and T we give the semi-major axes of orbits of the planets calculated by the TBmod model $(N' + 4)/10$ and the period computed by the way of the Third Law of Kepler, respectively. In Columns a_p and T_p we present the astronomical values of the observed orbital parameters. In the last two columns we give the determination of the error between the computed heliocentric distances and the astronomical ones Δa and ΔT , where the values tending to zero indicate a good degree of certainty.

planetary objects. Patton (1988) obtained the TB Law for Lagrange multipliers and applied it with acceptable results to eleven large asteroids. Through the approach of Monte Carlo, Lynch (2003) concluded that it is not possible to assure that the Titius-Bode Law explains the distribution of planets and satellites and Chang (2008) found that the distribution of the ratio of rotational periods in the 55 Cnc system is apparently inconsistent with that derived from the Titius-Bode Law. More recently Kotliarov (2009) has presented an interesting discussion of the Butusov model and proposed a generating function for the distribution of the planets.

2. MODIFIED TITIUS-BODE LAW

We propose a modification to the Titius-Bode Law (TBmod) by combining the sequences X (0, 0, 3, 6, 12, 24, 48, 96, 192, 288, 384, 576, 960, 1728) and X' (0, 3, 3, 6, 12, 24, 48, 96, 96, 96, 192, 384, 768, 1536), which were derived empirically by García Guerra (2005). The sum of the sequences $N' = X + X'$ reproduces one by one the terms of the succession of Titius-Bode (TB) from Mercury to Pluto, including the approach to the asteroid Ceres and other distant planetary objects. The semi-major

axes of the planets are derived from the modified TB formulation $a = (N' + 4)/10$ which shows the curvilinear distribution of distances for each one of them (Figure 1). We presented the exponential function fit $r = e^{0.6122x-2.8176}$, $R^2 = 0.9990$ obtained from the interpolation ($r = Ae^{x/t}$) and we compared it with the semi-major axes of major planetary bodies and other small objects, among them Ceto, Eris, Sedna and the distant object SQ372.

In Table 1 we display the orbital parameters a and T calculated with the TBmod model, and the data for a_p and T_p (Astronomical Almanac 2010); in the columns $\Delta a = (a_n - a_p)/a_p$ (Kotliarov 2008) and $\Delta T = (T_n - T_p)/T_p$ we give the proportionality ratios between the calculated and observed values to measure the degree of certainty, which is considered acceptable if their values are close to zero. In our case these TBmod ratios have values of less than 5% and 8% respectively. One of our goals is to determine some kind of mathematical expression that would represent the general TBmod behavior, and to compare it with tendencies that show the different models deduced from the TB law summarized in Table 2.

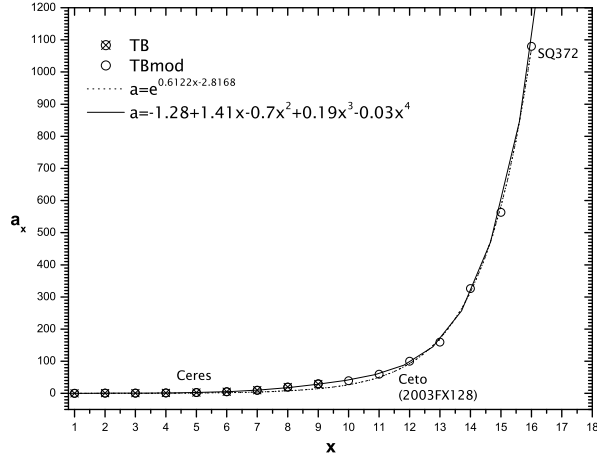


Fig. 1. Distribution of the semi-major axes of the planets and some small objects, given by the original and modified Titius-Bode Law, TB and TBmod respectively. We also present two interpolations that summarize the combination with an exponential function ($r = Ae^{x/t}$) and a seventh order polynomial (we only display the five first terms of the series), showing interpolated fits from Neptune to the interior region of the Kuiper Band.

Given the sequence of N' integer numbers; we carry out a setup of numerical operations in order to construct a function 2^n , which leads us to write this sequence like multiples of the common factor $3 \cdot 2^5$ whose first value $N' = 0$ for $n = 1$ (Mercury) we took into account in the discussion even though it does not exactly reproduce value the 0.387 of Mercury (Table 1). The resulting equations are:

$$r_n = 0.4 + 9.6 \cdot 2^{n-7}, \quad n \leq 8 \quad (1)$$

$$r_n = 29.2, \quad n = 9 \quad (2)$$

$$r_n = 29.2 + 9.6 \cdot \sum_{i=10}^n 2^{i-10}, \quad n \geq 10 \quad (3)$$

If we arrange the elements $n = 9$ and $n \geq 9$ we realize that they constitute the total sum of the geometric progression given by $(2^{n-9} - 1)$, so that eventually we obtain the modified TBmod model, governed by two generic intervals of arithmetic and geometric progressions, respectively

$$r_n = 0.4 + 9.6 \cdot 2^{n-7}, \quad n \leq 8 \quad (4)$$

$$r_n = 19.6 + 9.6 \cdot 2^{n-9}, \quad n \geq 9 \quad (5)$$

Among the distributions of planetary bodies shown in Table 1 we observed that they present tendencies in the internal region of the Solar System including the TBmod distribution (Figure 2), although some of them diverge for the outer planets and even

TABLE 2
SOME MODELS THAT FIT THE
TITIUS-BODE LAW

Titius-Bode Model	Reference
$r_n = 0.3 + 0.3 \cdot 2^n$ $n = -1, 0, 1, 2, \dots, 6$	Wurm (1803) ^a
$r_n = 0.2792 \cdot 1.53^n$ $n = 1, 2, 3, \dots, 11$	Armellini (1921) ^a
$r_n = 0.4 + 0.0075 \cdot 2^n$ $n = -1, 0, 1, 2, \dots, 6$	Nicolini (1957) ^a
$r_n = 0.2792 \cdot 1.52^n$ $n = 1, 2, 3, \dots, 11$	Munini & Armellini (1978) ^a
$r_n = 0.283 \cdot 1.52^n$ $n = 1, 2, \dots$	Badolati (1982)
$r_n = 0.4 + 0.3 \cdot 2^{(n-2)}$ $n = -\infty, 0, 1, 2, \dots, 9$	Holton & Brush (2001)
$r_n = e^{0.53074n-1.51937}$ $n = 0, 1, 2, 3, 4, \dots$	Ortiz et al. (2007)
$r_n = e^{0.5894n-1.65026}$ $n = -\infty, 0, 1, 2, \dots, 9$	Poveda & Lara (2008)
$r_n = e^{0.53707n-1.661}$ $n = -1, 0, 1, 2, \dots, 6$	Pankovic & Radakovic (2009)

^aAs cited by Badolati 1982.

more so for distant objects. Note that all the models have difficulty in reproducing the parameters of Mercury, so that historically it has been necessary to postulate special conditions for this planet; we shall see how to avoid this problem.

The actual distribution of the planets is contained in the TBmod curvilinear path, which coincides with the values of observed semi-major axes. We have chosen the logarithmic scale to better visualize the linear trace of the other six models. The Armellini and Bodolati model does not reproduce the distribution of planetary objects beyond Jupiter. The Nicolini and Holton & Brush models match the TBmod up to Uranus, as the Nicolini model is only for the planets. The Armellini and Bodolati models show values a_n that are very close. The case of the models of Wurm (not shown in Figure 2) falls short of all values Δa_n . In Ortiz et al. (2007), Poveda & Lara (2008), and Pankovic & Radakovic (2009) we observe that their traces exhibit a certain parallelism and proximity between the distribution of planetary objects. Finally, these cases including TBmod are those that best approximate the actual distribution of planetary objects. Of course the TBmod proposal shows the best approximation to the above mentioned distribution.

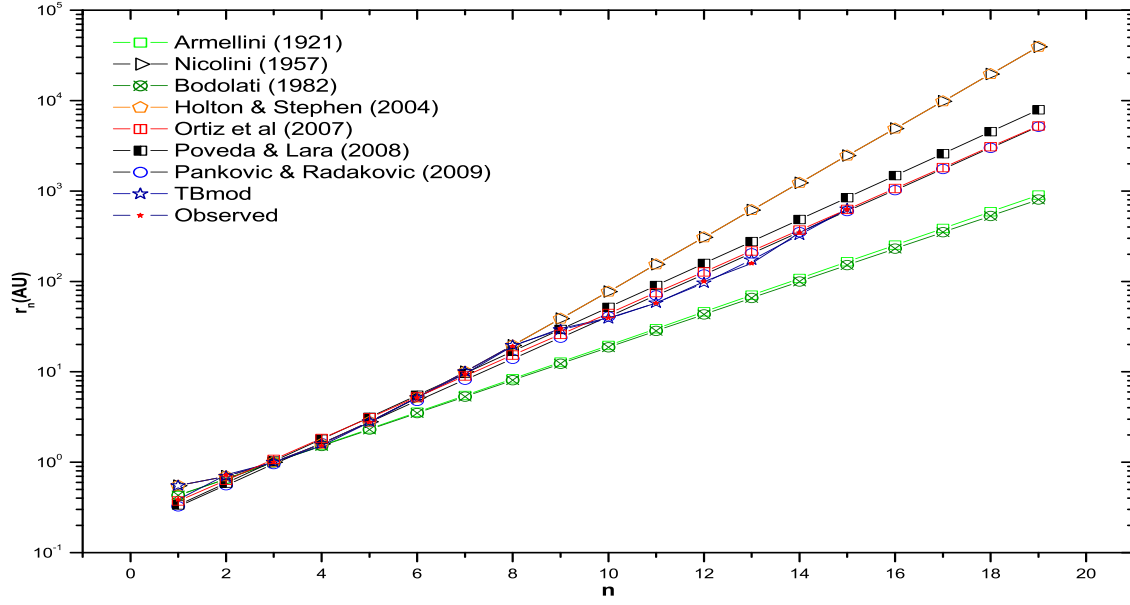


Fig. 2. Titius-Bode models of several authors including the TBmod variant proposed in this work. It is to be noted that the models are distributed above or below the real TB distribution of planets and the TBmod curvilinear path, which coincides with the values of the observed semi-major axes. We have chosen the logarithmic scale to better visualize the linear trace of the other six models. The color figure can be viewed online.

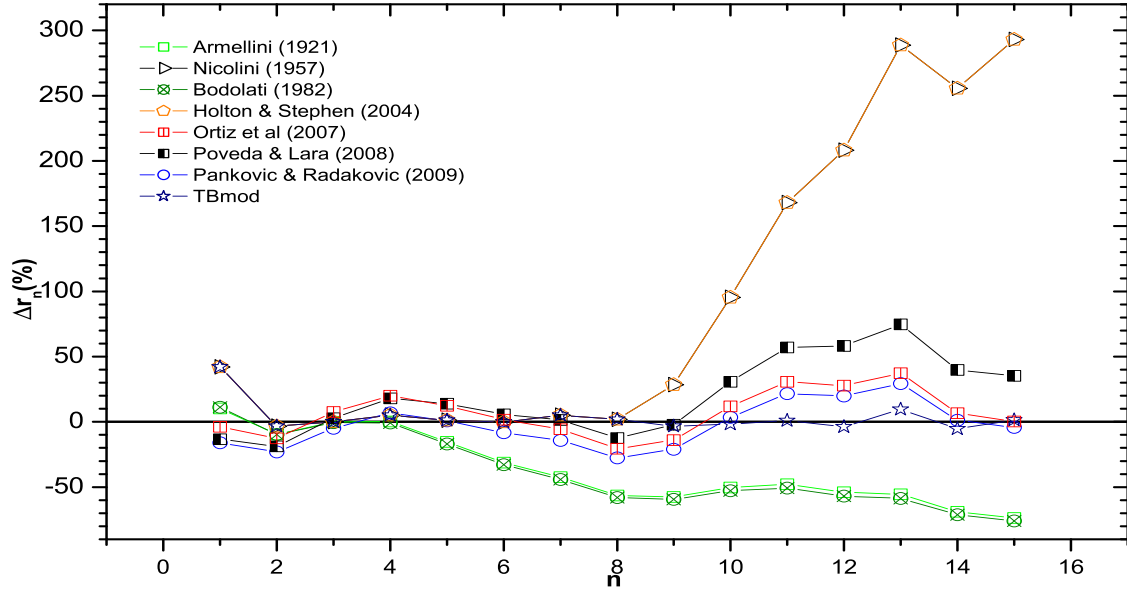


Fig. 3. The degree of certainty of the TB models proposed by various authors in terms of the ratio $\Delta a = (a_n - a_p)/a_p$. The color figure can be viewed online.

3. DEGREE OF CERTAINTY OF TBMOD

We realize that the modified TBmod model acceptably reproduces the orbital parameters a_n . We have examined the degree of certainty of the model

through the differences between the calculated parameters (a_n , T_n) and those observed (a_p , T_p) by the ratio $\Delta a = (a_n - a_p)/a_p$, and similarly by calculating the ratio $\Delta T = (T_n - T_p)/T_p$, where the periods are the parameters obtained from Kepler's

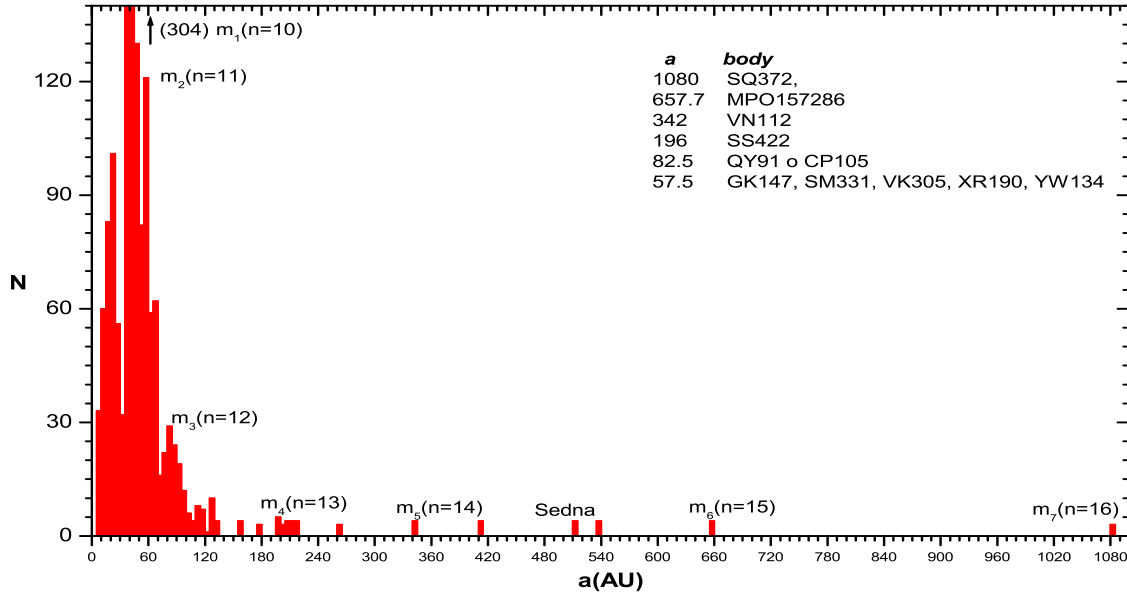


Fig. 4. Regions of accumulation in the Solar System of the small planetary bodies (taken from IAU Minor Planets Center: Observable Distant Minor Planets Orbital Elements). We observe that several of the small objects of the Solar System, like Eris, 2006HQ or Sedna, cannot be associated to the Titius-Bode Law. The color figure can be viewed online.

Third Law. If we apply this procedure to each of the models in Table 1 we will have an overview of the degree of certainty that the models possess as a whole.

The fit in Figure 3 shows the ratio between the values calculated for each model and the observed parameters. We can see that there are certain similarities up to the planet Saturn. However, there are divergences when we approach the outer regions of the Solar System. Note that the trace shows the smallest difference with the data for planetary objects due to the lower percentages of up to 10%. In this figure it is easy to identify the problem arising in all the models when reproducing the parameters of the planet Mercury; therefore it is normally avoided with an *ad hoc* number applied to this planet.

Another aspect that we want to emphasize is the fact that when general models are proposed what is implicitly done is to change the pattern of the sequence of integers for that of real numbers given by continuous functions $T = f(r)$. Thus, any Solar System object in principle will also fulfill this function and also the TB Law.

Given the large number of solar bodies now known we noticed that they fall on the semi-major axis distribution, although we know small objects like Eris, 2006HQ or Sedna that cannot be associ-

ated to the integers succession of the Titius-Bode Law. In the case of Ceres, which has historically been associated with the fifth place in the TB Law, we must say that we now know of the existence of a large number of other, smaller, planetary bodies whose orbital parameters are closer to the fifth place in Titius Bode's law.

With the intention of identifying the regions of the major accumulation of small planetary objects, we set ourselves the task of assembling the information (Figure 4) of IAU Minor Planets Center (Observable Distant Minor Planets Orbital Elements). We compare their semi-major axis accumulation points with the values corresponding to every integer n of the TBmod succession. The result indicates to us that only seven regions (m_1 , m_2 , m_3 , m_4 , m_5 , m_6 and m_7) can be associated with some integer 10, 11, 12 (2002TC30), 13 (Ceto), 14, 15 and 16 respectively, which makes us see the generic representation of the Titius Bode Law.

Another aspect that we want to review is whether the distribution of planets in our Solar System could be compared with that of extrasolar systems (often very different from ours), and so we enquired whether the TB model could be applied to such planetary systems.

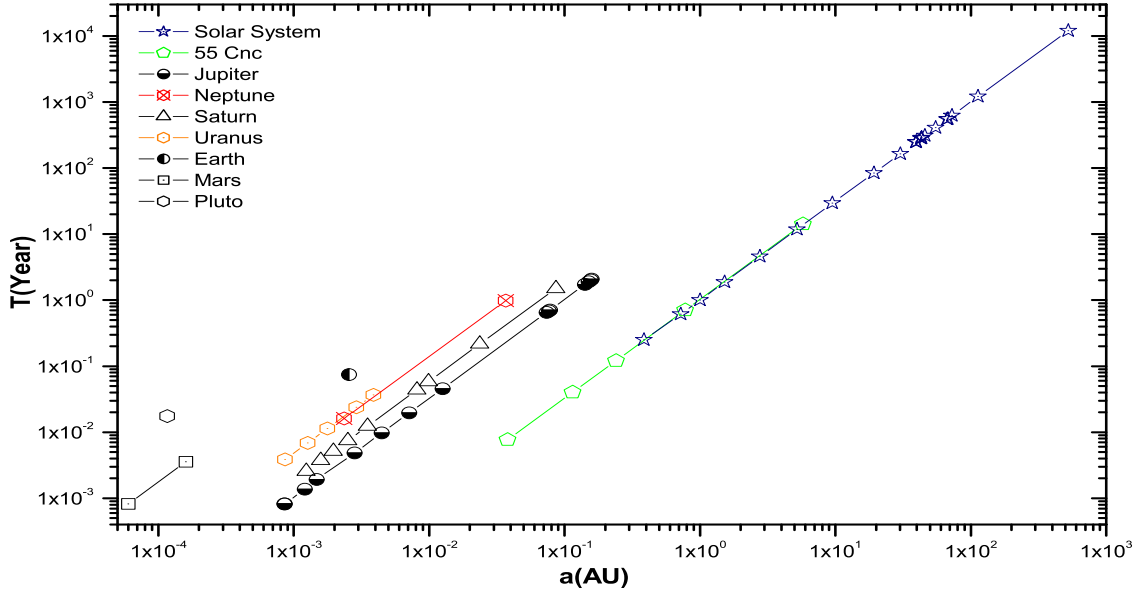


Fig. 5. Classification of planets and satellites. It shows the ranking of the Solar System and 55 Cnc, and satellite systems of planets. It is easy to see that 55Cnc and the Solar System are coincident because the masses of the central body are similar, but they differ clearly for the satellites. The color figure can be viewed online.

4. SYSTEMS OF SATELLITES AND EXOPLANETS

In the interpretation of the Titius-Bode Law a perennial concern has existed about its application to satellite systems that orbit the planets of our Solar System and, more recently, to planetary systems orbiting other stars such as ν And, 55 Cnc, 61 Vir, HD69830, HD181433, Gliese 876 and G1581 (data from Schneider 2010³). Of course, we must recognize the importance of characterizing the orbital period of the planetary objects under study by applying Kepler's Third Law $a^3/T^2 = K$, where $K = \pi^2 G(M + m)$ is called the Proportionality Kepler Parameter (Tables 3 and 4); we must have a clear idea that a self-gravitating system is characterized by means of its central mass and that this acts like a main factor of classification. This way, we observe in the fifth column that the values of $K[\text{m}^3 \text{s}^{-2}]$ are different for every self-gravitating system. Certainly this behavior is also estimated in the sixth column; the values of the ratio $a^3/T^2 = [\text{AU}^3 \text{yr}^{-2}]$ are of the order of one for our self-gravitating Solar System and 55Cnc, since both satisfy Kepler's proportionality. Finally, we must say that if the dimensionless ratio $(a^2/T^3)/K$ has fluctuations close

to one, then the parameters T , a , M and m are well-established.

Thus, also the systems of satellites of the planets are characterized in a unique way, although the constants of proportionality they obey have very small values (Figure 5); the extrasolar planets system possesses specific values of the above mentioned constant that differ or not from that of our Solar System, so much as mass of the star differs from the mass of the sun (Figure 6).

Now assume that the planetary systems 61 Vir and 55 Cnc obey our TBmod model. To reproduce the values of their semi-major axes, it is necessary to take the negative part of the integer numbers. We chose the values $-2, -1, 0, 1$ therefore obtaining TBmod values 0.01, 0.1, 0.2 and 0.3 respectively, among which it is easy to find the values of the semi-major axes of the planets of 55 Cnc and 61 Vir (Figure 7). Note that the objects 55Cnc(f) and 55Cnc(d) correspond to the planets Venus and Jupiter, respectively, and 61Vir(d) to a place between Mercury and Venus. This leads us to reassess the general functions proposed here for the Solar System, since the two equations do not allow us to calculate semi-major axes of less than 0.4. In order to avoid this problem we note that with the equation (4) we can determine these small values, and the remaining ones by means of

³<http://exoplanet.eu/catalog-all.php>.

TABLE 3
ORBITAL PARAMETERS OF SEVERAL PLANETARY OBJECTS AND THE SATELLITE SYSTEMS
OF THE PLANETS

		Object	a AU	T yr	m kg	K $\text{m}^3 \text{s}^{-2}$	a^3/T^2 $\text{AU}^3 \text{yr}^{-2}$	$a^3/T^2/K$
Sun	$M = 1.9891 \cdot 10^{30} \text{ kg}$	Mercury	0.387	0.251	$3.302 \cdot 10^{23}$	$3.120 \cdot 10^{18}$	0.9201	0.9273
		Venus	0.723	0.615	$4.869 \cdot 10^{24}$	$3.390 \cdot 10^{18}$	1.0006	1.0084
		Earth	1.000	1.000	$5.974 \cdot 10^{24}$	$3.390 \cdot 10^{18}$	1.0000	1.0078
		Mars	1.524	1.881	$6.419 \cdot 10^{23}$	$3.390 \cdot 10^{18}$	1.0005	1.0083
		Ceres	2.765	4.599	$9.500 \cdot 10^{20}$	$3.390 \cdot 10^{18}$	1.0000	1.0078
		Jupiter	5.203	11.862	$1.899 \cdot 10^{27}$	$3.390 \cdot 10^{18}$	1.0010	1.0079
		Saturn	9.509	29.458	$5.685 \cdot 10^{26}$	$3.360 \cdot 10^{18}$	0.9909	0.9984
		Uranus	19.251	84.013	$8.685 \cdot 10^{25}$	$3.430 \cdot 10^{18}$	1.0109	1.0187
		Neptune	30.188	164.749	$1.024 \cdot 10^{26}$	$3.440 \cdot 10^{18}$	1.0136	1.0215
		Pluto	39.499	248.430	$1.300 \cdot 10^{22}$	$3.380 \cdot 10^{18}$	0.9985	1.0063
		2002 TC302	55.096	410.620	$1.800 \cdot 10^{21}$	$3.360 \cdot 10^{18}$	0.9919	0.9997
		Eris	67.668	557.000	$1.700 \cdot 10^{22}$	$3.380 \cdot 10^{18}$	0.9987	1.0065
		2007 UK126	72.814	623.870	$7.100 \cdot 10^{20}$	$3.360 \cdot 10^{18}$	0.9919	0.9996
		2005 QU182	113.278	1210.530	$1.200 \cdot 10^{21}$	$3.360 \cdot 10^{18}$	0.9919	0.9997
		Sedna	524.453	12059.06	$7.200 \cdot 10^{21}$	$3.360 \cdot 10^{18}$	0.9920	0.9997
Jupiter	$M = 1.8990 \cdot 10^{27} \text{ kg}$	Metis	0.0009	0.0010	$9.4900 \cdot 10^{16}$	$3.2102 \cdot 10^{15}$	$9.210 \cdot 10^{-4}$	0.97240
		Adrasthea	0.0009	0.0010	$1.9000 \cdot 10^{16}$	$3.2102 \cdot 10^{15}$	$9.428 \cdot 10^{-4}$	0.99540
		Amalthea	0.0012	0.0010	$7.2200 \cdot 10^{18}$	$3.2102 \cdot 10^{15}$	$9.375 \cdot 10^{-4}$	0.98980
		Tebe	0.0015	0.0020	$7.6000 \cdot 10^{17}$	$3.2102 \cdot 10^{15}$	$8.707 \cdot 10^{-4}$	0.91920
		Io	0.0028	0.0050	$8.9400 \cdot 10^{22}$	$3.2103 \cdot 10^{15}$	$9.464 \cdot 10^{-4}$	0.99910
		Europa	0.0045	0.0100	$4.8000 \cdot 10^{22}$	$3.2102 \cdot 10^{15}$	$9.465 \cdot 10^{-4}$	0.99920
		Ganymede	0.0071	0.0200	$1.4820 \cdot 10^{23}$	$3.2104 \cdot 10^{15}$	$9.470 \cdot 10^{-4}$	0.99970
		Callisto	0.0126	0.0460	$1.0760 \cdot 10^{23}$	$3.2103 \cdot 10^{15}$	$9.470 \cdot 10^{-4}$	0.99980
		Leda	0.0740	0.6540	$5.7000 \cdot 10^{15}$	$3.2102 \cdot 10^{15}$	$9.472 \cdot 10^{-4}$	1.00000
		Himalia	0.0765	0.6860	$9.4900 \cdot 10^{18}$	$3.2102 \cdot 10^{15}$	$9.523 \cdot 10^{-3}$	1.00530
		Lisisthea	0.0781	0.7100	$7.6000 \cdot 10^{16}$	$3.2102 \cdot 10^{15}$	$9.471 \cdot 10^{-4}$	0.99990
		Elara	0.0783	0.7110	$7.6000 \cdot 10^{17}$	$3.2102 \cdot 10^{15}$	$9.476 \cdot 10^{-4}$	1.00040
		Ananque	0.1413	1.7280	$3.8000 \cdot 10^{16}$	$3.2102 \cdot 10^{15}$	$9.459 \cdot 10^{-4}$	0.99860
		Carne	0.1507	1.8950	$9.4900 \cdot 10^{16}$	$3.2102 \cdot 10^{15}$	$9.528 \cdot 10^{-3}$	1.00590
		Pasiphae	0.1567	2.0120	$1.9000 \cdot 10^{17}$	$3.2102 \cdot 10^{15}$	$9.495 \cdot 10^{-4}$	1.00250
		Sinophe	0.1580	2.0750	$7.6000 \cdot 10^{16}$	$3.2102 \cdot 10^{15}$	$9.158 \cdot 10^{-4}$	0.96680
Saturn	$M = 5.97 \cdot 10^{26} \text{ kg}$	Mimas	0.0012	0.0030	$3.7500 \cdot 10^{19}$	$1.0100 \cdot 10^{15}$	$3.00 \cdot 10^{-4}$	0.95350
		Enceladus	0.0016	0.0040	$1.0800 \cdot 10^{20}$	$1.0100 \cdot 10^{15}$	$3.00 \cdot 10^{-4}$	0.95170
		Tethys	0.0020	0.0050	$1.0240 \cdot 10^{20}$	$1.0100 \cdot 10^{15}$	$3.00 \cdot 10^{-4}$	0.95170
		Dione	0.0025	0.0070	$1.0950 \cdot 10^{21}$	$1.0100 \cdot 10^{15}$	$3.00 \cdot 10^{-4}$	0.95170
		Rhea	0.0035	0.0120	$2.3060 \cdot 10^{21}$	$1.0100 \cdot 10^{15}$	$3.00 \cdot 10^{-4}$	0.95150
		Titan	0.0082	0.0440	$1.3450 \cdot 10^{23}$	$1.0100 \cdot 10^{15}$	$3.00 \cdot 10^{-4}$	0.95140
		Hiperion	0.0099	0.0580	$1.7100 \cdot 10^{19}$	$1.0100 \cdot 10^{15}$	$3.00 \cdot 10^{-4}$	0.94960
		Iapetus	0.0237	0.2170	$1.8800 \cdot 10^{21}$	$1.0100 \cdot 10^{15}$	$3.00 \cdot 10^{-4}$	0.94990
		Febe	0.0864	1.5070	$3.9800 \cdot 10^{17}$	$1.0100 \cdot 10^{15}$	$3.00 \cdot 10^{-4}$	0.95090
Uranus	$M = 8.69 \cdot 10^{25} \text{ kg}$	Miranda	0.0009	0.0040	$6.5900 \cdot 10^{19}$	$1.4700 \cdot 10^{14}$	$4.2800 \cdot 10^{-5}$	0.99000
		Ariel	0.0013	0.0070	$1.3500 \cdot 10^{21}$	$1.4700 \cdot 10^{14}$	$4.3300 \cdot 10^{-5}$	1.00000
		Umbriel	0.0018	0.0110	$1.2000 \cdot 10^{21}$	$1.4700 \cdot 10^{14}$	$4.3300 \cdot 10^{-5}$	1.00000
		Titania	0.0029	0.0240	$3.5000 \cdot 10^{21}$	$1.4700 \cdot 10^{14}$	$4.3300 \cdot 10^{-5}$	1.00000
		Oberon	0.0039	0.0370	$3.0140 \cdot 10^{21}$	$1.4700 \cdot 10^{14}$	$4.3300 \cdot 10^{-5}$	1.00000
Neptune	$M = 1.03 \cdot 10^{26} \text{ kg}$	Triton	0.0024	0.0160	$1.34 \cdot 10^{23}$	$1.7400 \cdot 10^{14}$	$5.04 \cdot 10^{-5}$	0.98000
		Nereida	0.0368	0.9860	$2.06 \cdot 10^{19}$	$1.7400 \cdot 10^{14}$	$5.10 \cdot 10^{-5}$	1.00000
Earth	$M = 5.97 \cdot 10^{24} \text{ kg}$	Luna	0.0026	0.0750	$7.3480 \cdot 10^{22}$	$1.0200 \cdot 10^{13}$	$3.0100 \cdot 10^{-6}$	1.00000
Mars	$M = 6.42 \cdot 10^{23} \text{ kg}$	Fobos	0.0001	0.0010	$9.6300 \cdot 10^{15}$	$1.0900 \cdot 10^{12}$	$3.2000 \cdot 10^{-7}$	1.00000
		Deimos	0.0002	0.0040	$1.9300 \cdot 10^{15}$	$1.0900 \cdot 10^{12}$	$3.2000 \cdot 10^{-7}$	1.01000
Pluto	$M = 1.30 \cdot 10^{22} \text{ kg}$	Charon	0.0001	1.5200	$0.0170 \cdot 10^{21}$	$2.4500 \cdot 10^{10}$	$5.2000 \cdot 10^{-9}$	0.72000

In the first, second, third, and fourth columns, the names of the bodies, the major semi-axes, their periods and their respective masses, are given. In the fifth and the sixth columns the values of the proportionality parameter of Kepler for each body, and the quotient are given, and finally, in the seventh column we give the quotient of these parameters of proportionality whose value is very near to one.

TABLE 4
ORBITAL PARAMETERS OF THE EXOPLANETARY SYSTEM GLIESE 876, G1581,
 ν AND, 55 CNC, HD160691, HD69830 AND 61 VIR

Object	M kg	a AU	T yr	m kg	K $\text{m}^3 \text{s}^{-2}$	$a^3 T^{-2}$ $\text{AU}^3 \text{yr}^{-2}$	$a^3 T^{-2}/K$
ν And	$2.525 \cdot 10^{30} \text{ kg}$	1	0.059	0.01	$1.3100 \cdot 10^{27}$	$4.27 \cdot 10^{18}$	1.29
		2	0.822	0.65	$22.0036 \cdot 10^{27}$	$4.31 \cdot 10^{18}$	1.31
		3	2.550	3.57	$19.5356 \cdot 10^{27}$	$4.30 \cdot 10^{18}$	1.30
55Cnc	$1.97 \cdot 10^{30} \text{ kg}$	1	0.038	0.01	$0.0456 \cdot 10^{27}$	$3.36 \cdot 10^{18}$	0.92
		2	0.115	0.04	$1.5644 \cdot 10^{27}$	$3.36 \cdot 10^{18}$	0.95
		3	0.240	0.12	$0.3209 \cdot 10^{27}$	$3.36 \cdot 10^{18}$	0.94
		4	0.781	0.71	$0.2734 \cdot 10^{27}$	$3.36 \cdot 10^{18}$	0.94
		5	5.770	14.29	$7.2808 \cdot 10^{27}$	$3.37 \cdot 10^{18}$	0.94
61 Vir	$1.8890 \cdot 10^{30} \text{ kg}$	1	0.050	0.01	$0.0304 \cdot 10^{27}$	$3.19 \cdot 10^{18}$	0.95
		2	0.218	0.10	$0.1088 \cdot 10^{27}$	$3.19 \cdot 10^{18}$	0.95
		3	0.476	0.34	$0.1367 \cdot 10^{27}$	$3.19 \cdot 10^{18}$	0.95
HD69830	$1.71 \cdot 10^{30} \text{ kg}$	1	0.079	0.02	$0.0627 \cdot 10^{27}$	$2.89 \cdot 10^{18}$	0.86
		2	0.186	0.09	$0.0721 \cdot 10^{27}$	$2.89 \cdot 10^{18}$	0.86
		3	0.630	0.54	$0.1101 \cdot 10^{27}$	$2.89 \cdot 10^{18}$	0.86
HD181433	$1.55 \cdot 10^{30} \text{ kg}$	1	0.080	0.03	$0.0452 \cdot 10^{27}$	$2.62 \cdot 10^{18}$	0.78
		2	1.760	2.63	$1.2150 \cdot 10^{27}$	$2.62 \cdot 10^{18}$	0.79
		3	3.000	5.95	$1.0252 \cdot 10^{27}$	$2.62 \cdot 10^{18}$	0.76
Gliese876	$1.55 \cdot 10^{29} \text{ kg}$	1	0.021	0.01	$0.0399 \cdot 10^{27}$	$1.12 \cdot 10^{18}$	0.32
		2	0.130	0.08	$1.3559 \cdot 10^{27}$	$1.13 \cdot 10^{18}$	0.32
		3	0.208	0.17	$4.3202 \cdot 10^{27}$	$1.13 \cdot 10^{18}$	0.32
		4	0.334	0.34	$0.0873 \cdot 10^{27}$	$1.12 \cdot 10^{18}$	0.32
G1581	$6.16 \cdot 10^{29} \text{ kg}$	1	0.030	0.01	$0.0116 \cdot 10^{27}$	$1.04 \cdot 10^{18}$	0.36
		2	0.041	0.01	$0.0934 \cdot 10^{27}$	$1.04 \cdot 10^{18}$	0.32
		3	0.070	0.04	$0.0320 \cdot 10^{27}$	$1.04 \cdot 10^{18}$	0.27
		4	0.220	0.18	$0.0424 \cdot 10^{27}$	$1.04 \cdot 10^{18}$	0.32

In the Columns 1 to 5, the names of the bodies, the mass of the star, the major semi-axes, their periods and the planet masses, are given. In Columns 6 and 7 the values of the proportionality parameter of Kepler for each body, and the quotient are given, and finally, in Column 8 we give the quotient of these parameters of proportionality, whose value is very close to one.

the following equations (TBF):

$$r_n = 0.008 + 9.6 \cdot 2^{n-6}, \quad -4 \leq n < 2 \quad (6)$$

$$r_n = 0.4 + 9.6 \cdot 2^{n-7}, \quad 2 \leq n < 9 \quad (7)$$

$$r_n = 19.6 + 9.6 \cdot 2^{n-9}, \quad n \geq 9 \quad (8)$$

Now we present the distribution of the objects that induces each of the equations (6–8) in order to discern their tendencies and to display the intervals that are valid in each (the values of χ^2 for each interval are 0.002, 0.241 and 0.379 respectively). It is obvious that there are three regions bound by the intersection of the equations (6) and (7), and equations (7) and (8) (Figure 8) and whose approximate values are found to be $(n_1, r_1) = (2.5, 0.8 \text{ AU})$ and $(n_2, r_2) = (8.4, 26.5 \text{ AU})$, respectively. This suggests that these three intervals delimit the regions

between the Sun and Venus, inside the region of the hypothetical vulcanoid objects that contains Mercury, between Major Solar Bodies but without Mercury, and finally from Neptune to the regions of the outer Solar System, into which we have included the accumulation points $(m_1, m_2, m_3, m_4, m_5, m_6$ and $m_7)$.

Taking equations (6–8) we have determined the values of the semi-major axes and have fitted exponential functions (values of R^2 as 0.9999, 0.9971 and 0.9999 respectively):

$$r = e^{0.63413x-1.81942}, \quad x < 2 \quad (9)$$

$$r = e^{0.67115x-2.38121}, \quad 2 \leq x < 9 \quad (10)$$

$$r = e^{0.68879x-3.89173}, \quad x \geq 9 \quad (11)$$

Since equation (9) represents the vulcanoid objects we wish to compare it with the semi-major axes

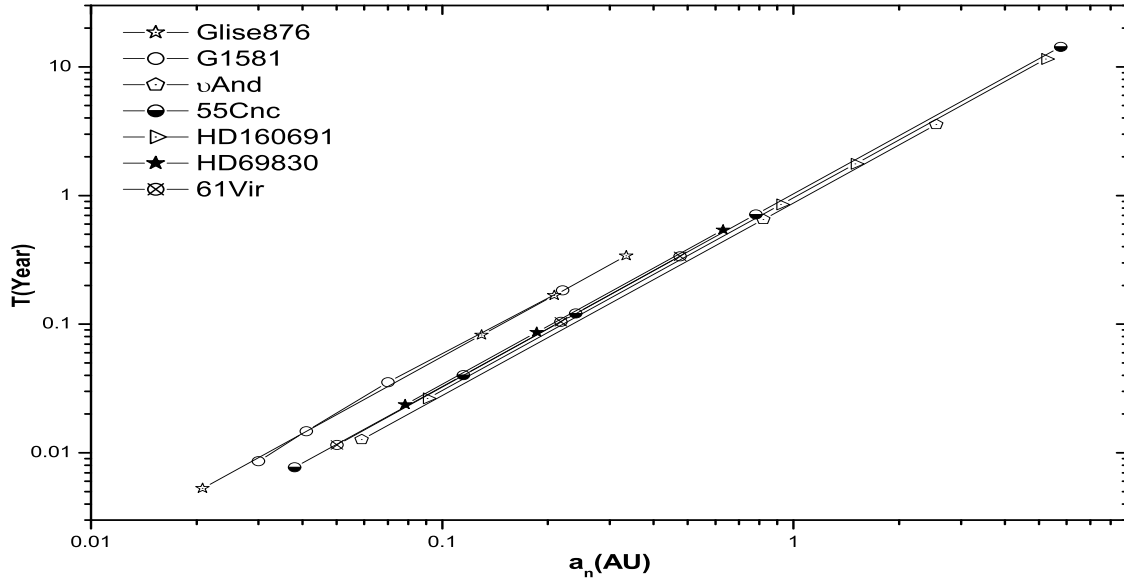


Fig. 6. Orbital parameters of the exoplanetary system. Observe that the systems whose central masses are similar to that of the Sun are *v* And, 55 Cnc, 61 Vir, HD 69830 and HD 181433, and differ from those of Gliese 876 and Gliese 1581.

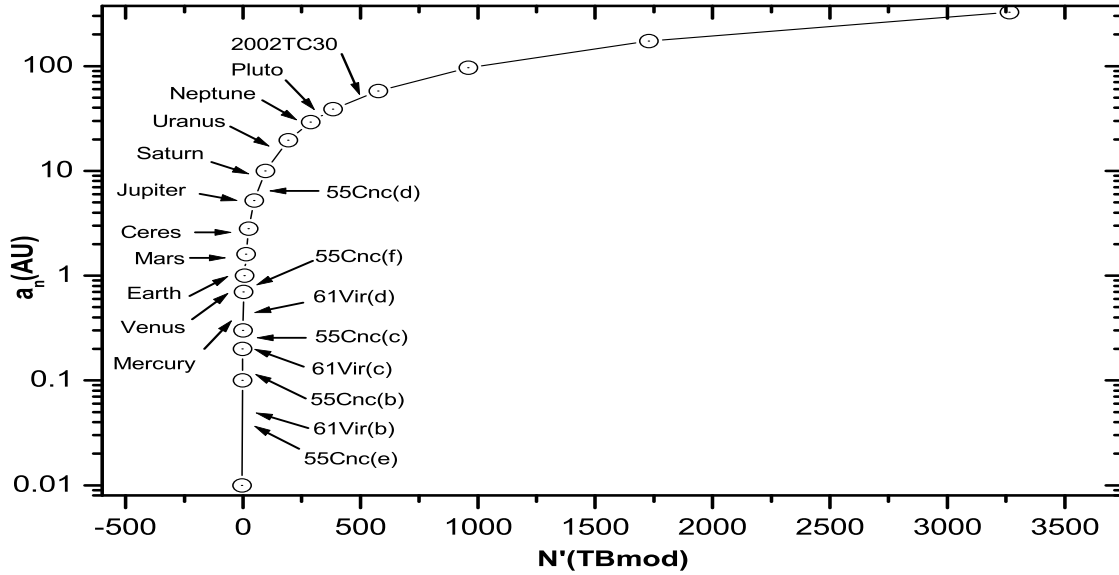


Fig. 7. Distribution of exoplanets of 55 Cnc and 61 Vir. As the central mass of both systems is similar to that of the Sun, we will assume that they satisfy the equations we have called TBF. We include the members of the Solar System with the purpose of comparing the extrasolar objects with those familiar to us. On the abscissa axis we give the heliocentric distances of the planetary objects according to the order of the integer succession TB law.

of the exoplanets (Schneider 2010)⁴ known until now. We have found that some accumulation points correspond to certain elements of TBF (Figure 9). Nevertheless, it is not possible to represent the totality

⁴<http://exoplanet.eu/catalog-all.php>.

of them. Another interesting aspect is the concentration of vulcanoid objects around $n = -2$. Perhaps it is due to the existence of the protoplanetary wall near a central mass recently analyzed (Calvet, D'Alessio, & Woolum 2005), whose radius of subli-

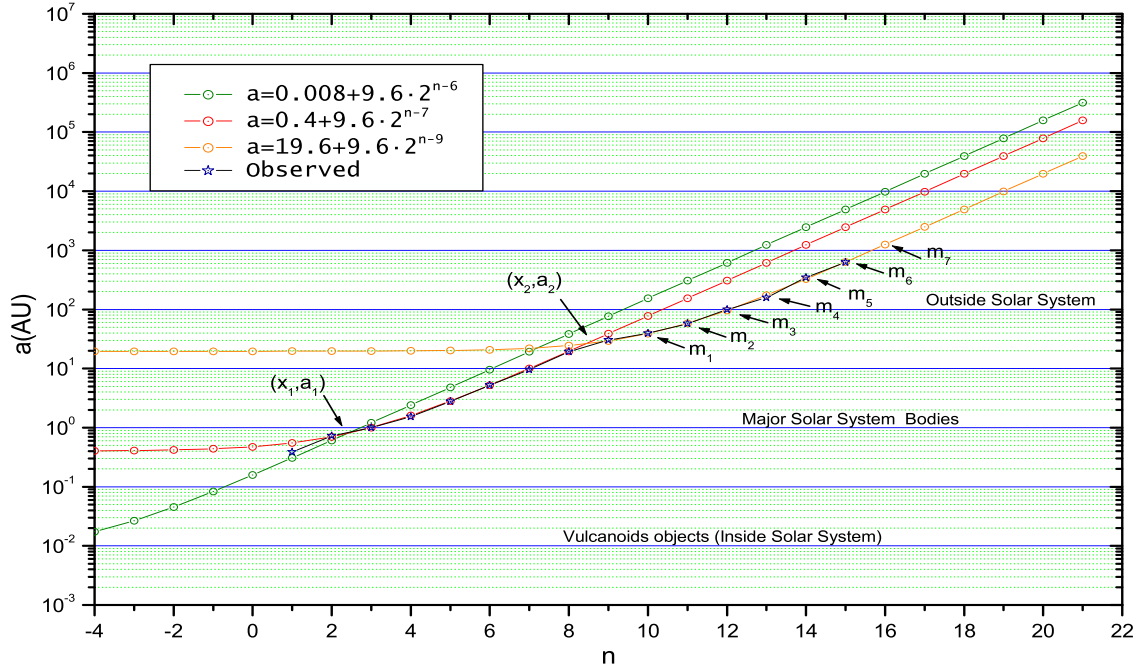


Fig. 8. Distribution of the planetary objects in three regions defined by the intersections of the functions. The intersection of the first two, assuming them as continuous functions, defines the point $(n_1, a_1) = (2.5, 0.8 \text{ AU})$, and the intersection of the second and the third ones gives the points $(n_2, a_2) = (8.4, 26.5 \text{ AU})$. Through these points the three regions of the Solar System are defined and it is possible to apply them to extrasolar systems with central masses similar to those of the Sun, 55 Cnc and 61 Vir. We include the accumulation points ($m_1, m_2, m_3, m_4, m_5, m_6$ and m_7). The color figure can be viewed online.

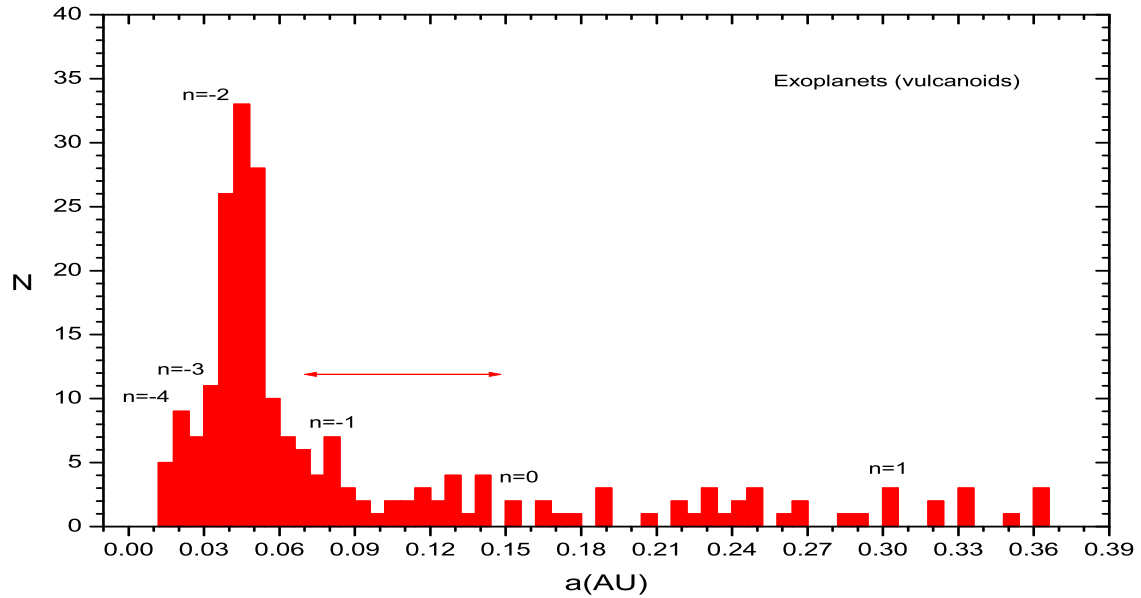


Fig. 9. Exoplanets with semi-major axes less 0.39 AU. The color figure can be viewed online.

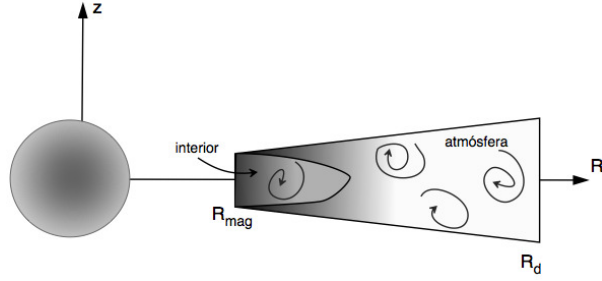


Fig. 10. A simplified distribution of a protostellar turbulent disk model to give an idea of how annular regions can form in such a disk.

mation we identify with the red color line between 0.07 and 0.15 AU.

Perhaps the origin of these regions can be found in the early formative stages of the protoplanetary disk dominated by turbulent forces that led to the formation of ring band regions (annular regions). With time, these regions evolved, and were confined into bands by the presolar material. The planets would have been formed as a result of the agglomeration of small particles into larger ones. A hydrodynamic vision has been included in the recent model of Adame (2010), who describes a turbulent protostellar disk (Figure 10) with central small masses. Here we can see certain criteria for the formation of annular regions; for example, it is possible to consider that the origin of the TBF distribution arises from a stationary wave system, according to the initial conditions, the mass of the central body being the main parameter.

5. FINAL COMMENTS AND CONCLUSIONS

We have studied the general structure of the Solar System through the Titius-Bode Law, which we have applied to the exoplanets system. It has lead to us to consider that the TBF distribution of planetary objects (equations (6–11)) occurs in three great groups: Inner Solar System bodies, Major Solar System bodies and Outer Solar System bodies. For the case of Mercury ($n = 1$) we improved the determination of the semi-major axis. The order of the major objects agrees well with the integer TBF sequence, including the accumulation region ($n = 5$) represented by Ceres or the asteroid belt. In the outer Solar System, where objects with very eccentric orbits are located, we observed that the TBF integers are associated mainly to regions of accumulation of small agglomerations with values $n = 15$ or 16 , and to the abundant concentrations of small objects for $n = 10, 11$ or 12 .

If we consider solely those systems with central masses similar to the Sun, i.e., 55 Cnc, 61 Vir and HD69830, we can assign to certain objects values n of TBF (vulcanoids and major objects) according to equations (6–8) and Table 4. For example, 55Cnc(1) with $n = -2$, 61Vir(1) with $n = -2$, HD69830(1) with $n = -1$, and HD69830(2) with $n = 0$.

With the set of equations (equations 6–11) we can see the general orbital behavior of Solar System bodies, which appears to contain the final status of the presolar cloud processes from the stage of protoplanetary disk to planet formation. Of course, any theory would have to include other phenomena, such as migration of planets (Masset 2008), or magnetohydrodynamic phenomena that may have occurred in our Solar System. In this context, when we think about the distribution of planets in the Solar System, we are actually considering the primitive physical conditions which dominated the presolar cloud which created regions of the protoplanetary ring from which the planets were created after a process of accretion of the particles that formed these protoplanetary rings.

We have speculated that the TBF distribution arose from a stationary wave system in the presolar cloud where it induced the formation of certain annular regions, simultaneously generating turbulent accretion phenomena. On the other hand, we imagine that these conditions differ from other protoplanetary environments where the distribution and size of such rings would be subject to different chemical composition, shape, distribution and laws of accretion of the solid bodies.

We thank the referee for useful comments which improved our presentation.

REFERENCES

- Adame, L. 2010, PhD Thesis, Universidad Nacional Autónoma de México, Mexico
- Badolati, E. 1982, Moon and the Planets, 26, 339
- Calvet, N., D'Alessio, P. D., & Woolum, D. S. 2005, in ASP Conf. Ser. 341, Chondrites and the Protoplanetary Disk, ed. A. N. Krot, E. R. D. Scott, & B. Reipurth (San Francisco: ASP), 353
- Chang, H. Y. 2008, J. Astron. Space Sci., 25, 239
- García Guerra, C. 2005, Distancias Planetarias (Mexico: SEP; Registro Público de Derechos de Autor 03-2005-081713522000-01, 25 agosto 2005)
- Holton, G. J., & Brush, S. G. 2001, Physics, the Human Adventure: from Copernicus to Einstein and Beyond (3rd ed.; New Brunswick, N. J.: Rutgers Univ. Press)
- Horedt, G. P., Pop, P., & Ruck, H. 1977, Celest. Mech., 16, 209

- Jaki, S. L. 1972, *Am. J. Phys.*, 40, 1014
 Kotliarov, I. 2008, *MNRAS*, 390, 1411
 ———. 2009, *arXiv:0807.0757v1*
 Lynch, P. 2003, *MNRAS*, 341, 1174
 Masset, F. S. 2008, in *IAU Symp. 249, Exoplanets: Detection, Formation and Dynamics*, ed. Y.-S. Sun, S. Ferraz-Mello, & J.-L. Zhou (Cambridge: Cambridge Univ. Press), 331
 Nieto, M. M. 1970, *A&A*, 8, 105
 ———. 1975, *Icarus*, 25, 171
 Ortiz, J. L., Moreno, F., Molina, A., Santos Sanz, P., & Gutiérrez, P. J. 2007, *MNRAS*, 379, 1222
 Ovenden, M. W. 1972, *Nature*, 239, 508
 ———. 1975, *Vistas Astron.*, 18, 473
 Patton, J. M. 1988, *Celest. Mech.*, 44, 365
 Pankovick, V., & Radakovick, A. 2009, *arXiv:0903.1732v1*
 Poveda, A., & Lara, P. 2008, *RevMexAA*, 44, 243

J. Daniel Flores-Gutiérrez: Instituto de Astronomía, Universidad Nacional Autónoma de México, Apdo. Postal 70-264, 04510 México, D. F., Mexico (daniel@astro.unam.mx).
 Carlos García-Guerra: Facultad de Arquitectura, Universidad Nacional Autónoma de México, Mexico (carlosgg2000@hotmail.com).